Pressure Effects on the Structure and Phase Behavior of DMPC-Gramicidin Lipid Bilayers: A Synchrotron SAXS and ^{2}H-NMR Spectroscopy Study

J. Eisenblätter and R. Winter
Department of Chemistry, Physical Chemistry I-Biophysical Chemistry, University of Dortmund, D-44227 Dortmund, Germany

ABSTRACT The influence of Gramicidin D (GD) incorporation on the structure and phase behavior of aqueous dispersions of DMPC lipid bilayers has been studied using small-angle x-ray scattering (SAXS) and ^{2}H-NMR spectroscopy. The experiments covered a temperature range from −10°C to 60°C and a pressure range of 0.001–4 kbar. Pressure was used to be able to tune the lipid bilayer conformational order and phase state and because high pressure is an important feature of certain natural biotopes. The data show that, depending on the GD concentration, the structure of the temperature- and pressure-dependent lipid phases is significantly altered by the insertion of the polypeptide, and a *p,T*-phase diagram could be obtained for intermediate GD concentrations. Upon gramicidin insertion, a rather narrow fluid-gel coexistence regions is formed. Two gel phases are induced which are different from those of the pure lipid bilayer system and which separate at low temperatures/high pressures. For both the temperature- and pressure-induced fluid-to-gel transition, a similar pseudocritical transitional behavior is observed, which is even more pronounced upon incorporation of the peptide.

INTRODUCTION

Understanding the interactions between lipid bilayers and peptides is an important issue of membrane biophysics and structural biology (1–4). Here, we report on studies of peptide-lipid interactions using small-angle x-ray scattering (SAXS) and ^{2}H-NMR spectroscopy. We investigated the effect of incorporation of ~1–4 mol % gramicidin D (GD) on the structure and phase behavior of aqueous suspensions of the fully hydrated, neutral DMPC (1,2-dimyristoyl-*sn*-glycero-3-phosphatidylcholine (di-$C_{14:0}$)) phospholipid bilayer in the temperature range of −10°C–60°C at pressures up to 4000 bar (400 MPa). Hydrostatic pressure is not only used as a physical parameter for studying the stability and energetics of biomolecular systems, but also because it is an important feature of certain natural membrane environments and the high pressure phase behavior of biomolecules is also of biotechnological interest (5–8). Compared to other biomolecules, lipid bilayers have been shown to respond most sensitively to hydrostatic pressure (5–17). Considerable knowledge exists about pressure effects on pure lipid bilayer systems; very little is known about lipid bilayer-peptide interactions under pressure, however (7,8,18–21). In this study, pressure was mainly applied so as to be able to finely tune the lipid chain lengths, conformation, and order parameters and to select specific lipid lamellar phases. ^{2}H-NMR spectral parameters were used to detect conformational changes upon incorporation of GD into the DMPC bilayer. Supplementary SAXS data yield information about changes in the lipid bilayer structure and phase behavior.

Biological ion channels are key molecules for cellular regulation and communication. The gramicidin family represents such a channel system in which specific changes in amino acid composition are to be correlated with cation binding selectivity and transport (22–26). A mixture of nine pentadecapeptids is produced naturally by the aerobic, sporulating bacterium *Bacilllus brevis*. The three major gramicidin species, A, B, and C, typically occur in a ratio of ~7:1:2, respectively, and have the amino acid sequence formyl-L-Val^1-D-Gly^2-L-Ala^3-D-Leu^4-L-Ala^5-D-Val^6-L-Val^7-D-Val^8-L-Trp^9-D-Leu^{10}-L-Xxx^{11}-D-Leu^{12}-L-Trp^{13}-D-Leu^{14}-L-Trp^{15}-ethanolamine, where Xxx is Trp in gramicidin A, Phe in gramicidin B, and Tyr in gramicidin C. As a consequence of the alternate L and D chirality, and all side chains being nonpolar, the peptide is able to adopt conformations of β-helices, which would be unacceptable for an all-L-amino acid peptide (21–25). A common form is the head-to-head dimer of two right-handed single-stranded β-helices. The conformation with 6.3 residues per turn ($\beta^{6.3}$-helix) is one of the possible active ion channel structures; it has a hydrophobic length of ~24 Å (channel diameter 4 Å) (Fig. 1 *a*). A further form is the left-handed antiparallel double-stranded $\beta^{5.6}$-helix, being ~31 Å long (Fig. 1 *b*), which has been observed in particular organic solvents and long-chain or gel phase lipid bilayer systems (17,21–23). For comparison, the hydrophobic fluid bilayer thickness is ~28 Å for DMPC bilayers (27,28), and the hydrophobic thicknesses of the gel phases are ~4 Å larger.

Even simple one-component phospholipid bilayers exhibit various phases, depending on the lipid configuration, level of hydration, ionic strength of the solvent, temperature, and pressure (3,11,27–30). At ambient pressure, four major types of thermotropic phases have been observed for saturated

Submitted July 1, 2005, and accepted for publication October 24, 2005.

Address reprint requests to Roland Winter, E-mail: winter@steak.chemie.uni-dortmund.de.

0006-3495/06/02/956/11 $2.00

doi: 10.1529/biophysj.105.069799

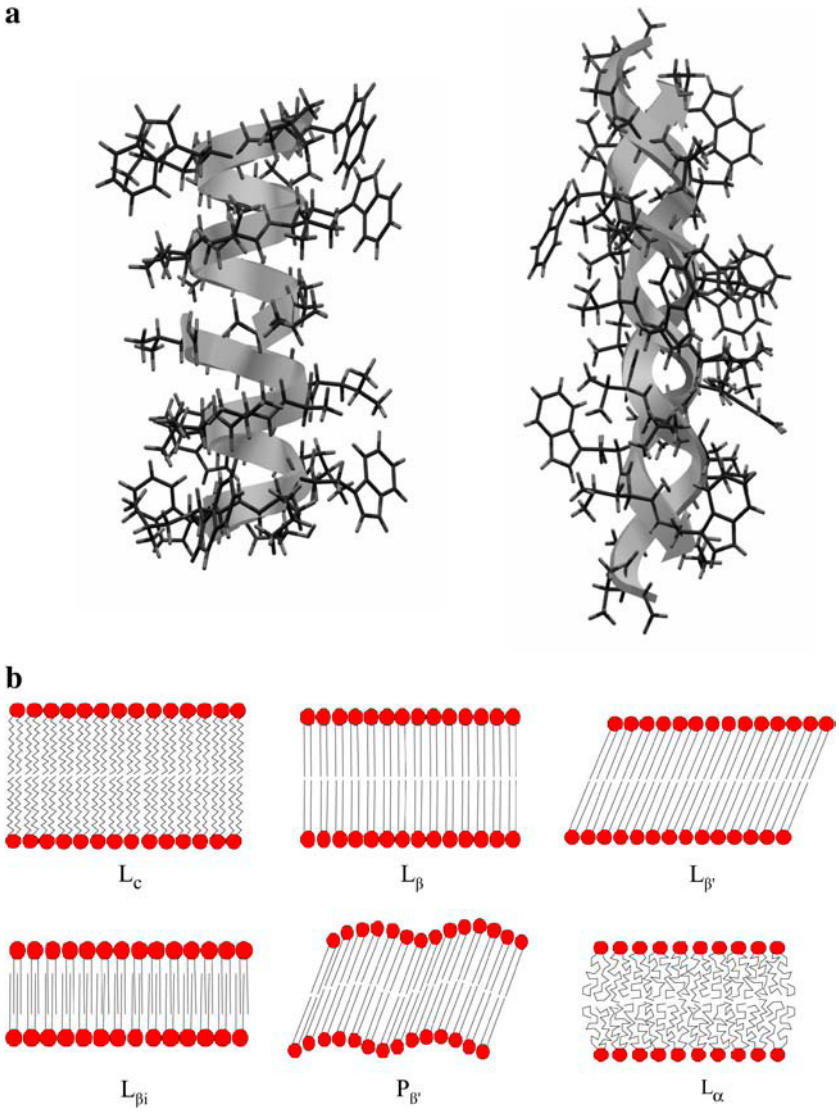

FIGURE 1 Schematic representation of (*a*) the dimeric single-stranded helical channel structure (*left*) and the ~6–7 Å longer double-stranded helical structure (*right*) of gramicidin. (*b*) Typical lamellar phospholipid phases that may be induced by changing temperature or pressure.

phosphatidylcholines. Common lamellar structures are shown in Fig. 1 *b*. In DMPC, below 15°C, the $L_{\beta'}$ gel phase is formed, in which the acyl chains are fully extended, packed in a distorted hexagonal lattice, and tilted with respect to the lipid bilayer normal. A crystalline L_c phase is formed from the metastable $L_{\beta'}$ gel phase after prolonged cooling at low temperature. At ~15°C, the transition from the L_c (or $L_{\beta'}$) to the $P_{\beta'}$-phase takes place, which has a two-dimensional lattice structure in which the lipid bilayers are distorted by a periodic ripple in the plane of the lamellae. Further increase of temperature leads to the formation of a liquid-crystalline L_α phase at the main phase transition temperature $T_m \approx 24$°C. In this fluid-like lipid phase, the hydrocarbon chains are conformationally disordered (''melted'') and undergo extensive *trans*/*gauche* isomerizations reminiscent of fluid hydrocarbon chains.

Besides these thermotropic phase transitions, a variety of pressure-induced lamellar phase transformations have been observed (9–17), and it has been demonstrated that temperature and pressure have noncongruent effects on the structural and phase behavior of these systems. For example, a partially interdigitated gel phase ($L_{\beta i}$, see Fig. 1 *b*) may be induced in a particular region of the *p*,*T*-phase space. For saturated phospholipids, the fluid-to-gel main transition temperature increases at a rate of $dT/dp \approx 20$°C/kbar with increasing pressure. The SAXS and ^{2}H-NMR data taken in this study reveal how the structure and phase behavior of the DMPC lipid bilayer system changes as a function of temperature, pressure, and peptide concentration.

EXPERIMENTAL

Sample preparation

DMPC was obtained from Sygena Lipids (Liestal, Switzerland), chain-perdeuterated d_{54}-DMPC from Avanti Polar Lipids (Alabaster, AL). Both substances were used without further purification. GD was purchased from

Sigma Chemical (Deisenhofen, Germany). DMPC-GD mixtures were prepared by codissolving the appropriate amounts in chloroform and vortex mixing the solution. The solvent was evaporated under a gentle nitrogen stream and then removed under vacuum using a Speed Vac Sc 110 (Savant, Farmingdale, NY) for at least 16 h. Fully hydrated dispersions were then prepared by adding doubly distilled water, heating the hydrated mixtures above the main phase transition temperature of the lipid, vortex mixing, and freezing the samples in liquid nitrogen. At least five freeze-thaw-vortex cycles were performed to yield a homogenous lipid suspension throughout the sample.

X-ray diffraction

SAXS experiments were performed at beam line A2 of the HASYLAB at DESY. The reciprocal spacings $s = (2/\lambda)\sin\theta$ (λ wavelength of radiation, 2θ scattering angle) were calibrated by the diffraction pattern of rat-tail collagen ($d = 640$ Å). The lamellar lattice constant d of the multilamellar lipid bilayer stacking can be deduced from the diffraction patterns with an accuracy of better than ± 1 Å using Bragg's equation. For the investigation of the DMPC-GD system at elevated pressures, a high pressure x-ray cell with flat diamond windows was used, suitable for studies up to pressures of 4 kbar at temperatures ranging up to 100°C (for details, see Winter and Czeslik (11)).

^{2}H-NMR

The temperature-dependent ^{2}H-NMR measurements were performed using a home-built NMR spectrometer at a resonance frequency of 55.2 MHz in a superconducting magnet operating at a magnetic field of 8.45 T. The samples were sealed in a glass tube and placed in the solenoid coil of the rf-circuit. Temperature was controlled with a continuous flow cryostat (Oxford Instruments, Oxfordshire, UK) cooled with liquid nitrogen to within ± 0.2°C. For the high pressure experiments, a probe made of a titanium alloy, Ti-6Al-4V, was constructed (31,32) which fits into the room-temperature bore of a wide-bore superconducting magnet, diameter 72 mm, operating at a magnetic field of 9.4 T. The samples were placed in a glass tube, fitted to the solenoid rf-coil, and closed with a flexible polymer foil to separate the sample from the pressurizing fluid (methylcyclohexane). The experimental setup allowed studies at pressures up to 4000 bar and temperatures ranging from 5°C up to 80°C. Temperature was controlled with water from a thermostat circulating through the jacket of the high-pressure probe and is accurate to within ± 0.5°C. A Bruker (Karlsruhe, Germany) MSL 400 spectrometer was used for the high pressure studies operating at a resonance frequency of 61.4 MHz. All deuteron NMR experiments were performed using the quadrupolar echo pulse sequence $\pi/2_x$-τ_1-$\pi/2_y$-τ_2-acquisition. The pulse lengths and pulse spacings were ~3–6 and 30–50 μs, respectively.

The measured ^{2}H-NMR spectra are powder spectra. In the fluid phase, perdeuterated lipids display ^{2}H-NMR spectra, which are superpositions of axially symmetric quadrupolar powder patterns of all n C-D bonds along the acyl chain (30–33). From the sharp edges, the quadrupolar splittings $\Delta\nu_Q^{(n)} = (3/4)(e^2qQ/h)S_{CD}^{(n)}$ can be obtained, where e^2qQ/h is the static quadrupole coupling constant for the deuterons in the C-D bonds, and the C-D bond order parameter S_{CD} for distinguishable deuterons can be calculated according to $S_{CD}^{(n)} = \langle 3\cos^2\theta_n - 1\rangle/2$. θ_n is the instantaneous angle between a given C-D bond vector and the axis of rotational symmetry of the molecules, i.e., the bilayer normal. The Pake doublets of the methyl and methylene groups can be assigned consecutively according to their increasing quadrupolar splittings (33–36).

In all phases studied, the first spectral moment M_1 of the ^{2}H-NMR spectra has also been calculated, which is proportional to the average chain orientational order parameter of the lipid acyl chains, $M_1 = 4\pi/(3\sqrt{3})\langle\Delta\nu_Q^{(n)}\rangle \propto \langle S_{CD}^{(n)}\rangle$. Knowing the chain order parameters $S_{CD}^{(n)}$ of the C-D segments n, their projections D_n along the membrane normal can be calculated within an appropriate statistical model for their orientational partition function (37,38). From the sum of all projections, the mean hydrocarbon chain length of a lipid monolayer, D_C, can be deduced. Knowing the volume of the entire hydrocarbon chain also allows calculation of the mean chain cross sectional area, $\langle A\rangle$ (37,38). For the pressure-dependent studies, the pressure dependence of V_{CH_2} also has to be taken into account using compressibility data (39,40).

RESULTS AND DISCUSSION

Synchrotron x-ray diffraction

The SAXS experiments were performed on pure DMPC suspensions and the DMPC-GD mixtures at ambient pressure as a function of temperature (from -1°C to 50°C) and at selected temperatures as a function of pressure. The first-order Bragg reflections were used to calculate the lamellar lattice constant d, which comprises the sum of the lipid bilayer thickness and the thickness of one adjacent interlamellar water layer. The diffraction patterns of the pure DMPC dispersions (Fig. 2 *a*) show the pretransition as well as the main lipid phase transition as a relatively sharp shift of the peak positions at ~15°C and 24°C, respectively. The lamellar lattice constant increases from ~60 Å in the $L_{\beta'}$-phase to ~66 Å in the ripple gel phase $P_{\beta'}$ of DMPC (Fig. 3 *a*). Due to the highly disordered chains in the fluid L_α-phase, the bilayer thickness decreases to a lattice constant of ~62 Å above 24°C (Fig. 3 *a*). If gramicidin is incorporated, the diffraction pattern changes drastically (Fig. 2, *b* and *c*). For example, in the DMPC-2.2 mol % GD sample, two different Bragg reflections can be distinguished below 17°C. The corresponding d-spacings are shown in Fig. 3 *a* as well. In the two-phase region, the d-spacings of the two gel phases are 60 and 71 Å, respectively. At higher temperatures, a single gel phase with a d-spacing of ~71 Å remains. The d-spacing in this gel phase is thus ~4 Å larger than that of the $P_{\beta'}$ phase of the pure DMPC bilayer. In the all-fluid lipid phase at $T > 25$°C, a d-spacing of 63–64 Å is measured, which is slightly (~1 Å) larger than that of the pure lipid L_α phase. Figs. 2 and 3 also contain data for the DMPC-4.4 mol % GD mixture. Here, no clear phase separation as indicated by a coexistence of two lamellar (001) Bragg peaks is observed at lower temperatures. Only one lamellar reflection with $d = 69$ Å is recorded in the gel phase region, which decreases with increasing temperature.

The lamellar lattice constants d of the DMPC-GD samples studied show that incorporation of GD leads to an extraordinarily large d-spacing in the gel phases. This swelling might be induced by the formation of longer, double helical forms of gramicidin in long-chain gel-type lipid bilayers or by the swelling of the interlamellar water. The former mechanism can probably be ruled out by recent Fourier transform infrared (FTIR) spectroscopic data (17), which showed that, in contrast to long-chain phospholipids-gramicidin mixtures with lesser hydrophobic coupling, the helical dimer structure of GD is prevailing in both fluid and gel phases of DMPC (18).

To explore the effect of pressure on the structure and phase behavior of the DMPC-polypeptide mixtures, we studied the pressure dependence of the SAXS diffraction patterns of

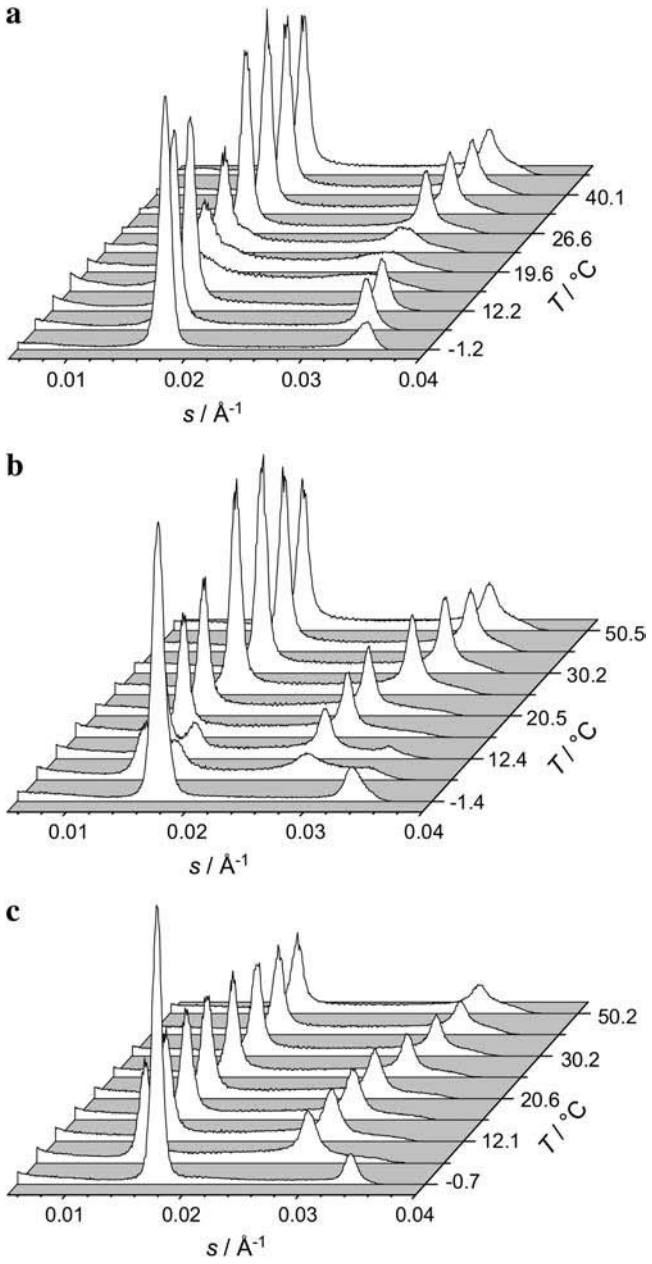

FIGURE 2 SAXS data of (*a*) DMPC (25 wt %), (*b*) DMPC-2.2 mol % GD, and (*c*) DMPC-4.4 mol % GD dispersions in excess water as a function of temperature at ambient pressure.

DMPC and the DMPC-GD mixtures at temperatures of 21°C and 37°C. In pure DMPC dispersions at 37°C (Fig. 4), a shift to lower scattering vectors together with a change in the lineshape is observed at ~500 bar, which is due to the pressure-induced L_α to $P_{\beta'}$ phase transition; the corresponding lamellar lattice constant increases from 62 to ~65 Å (Fig. 5). Further increase in pressure results in a decrease of the *d*-spacing and a further pressure-induced gel-to-gel phase transition around 2000 bar, leading to a decrease of the lamellar repeat period to $d \approx 57$ Å, which is almost insensitive to further pressure increase (Fig. 3 *b*).

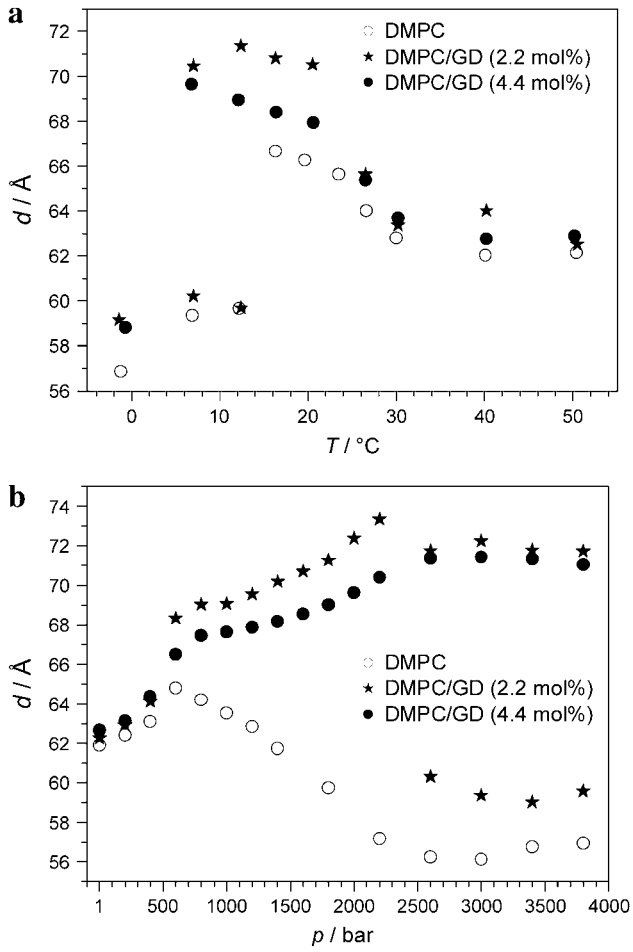

FIGURE 3 (*a*) Temperature dependence of the lamellar lattice constant *d* of DMPC lipid dispersions and the DMPC-GD mixtures at ambient pressure. (*b*) Pressure dependence of the lamellar lattice constant *d* of DMPC lipid bilayers and the DMPC-GD mixtures at $T = 37$°C.

The high pressure SAXS data of the DMPC-2.2 mol % GD mixture at 37°C are depicted in Fig. 4 *b*. The fluid phase is observed up to ~500 bar, where the fluid-to-gel transition occurs (Figs. 3*b* and 4*b*). A ripple gel phase is not found anymore, even at this low peptide concentration. The pressure dependence of the *d*-spacing has a different sign compared to the pure DMPC bilayer. It increases with increasing pressure, from 68.3 to 73.3 Å at 2200 bar. At higher pressures, a two-phase region is induced, probably a GD-rich (Gel′) and a GD-poor (Gel″) lipid-gel phase, which might be due to the increasingly hydrophobic mismatch between the lengths of the lipid chains and the polypeptide upon pressurization. The corresponding lattice constants of the Gel′ and Gel″ phases are 71 and 60 Å, respectively, and are insensitive to further pressurization of the system. A similar scenario holds for the DMPC-4.4 mol GD mixture. The high-pressure gel-gel phase transition occurs around 2600 bar for this system. The data thus clearly show that incorporation of gramicidin drastically changes the pressure-dependent gel phase behavior of DMPC.

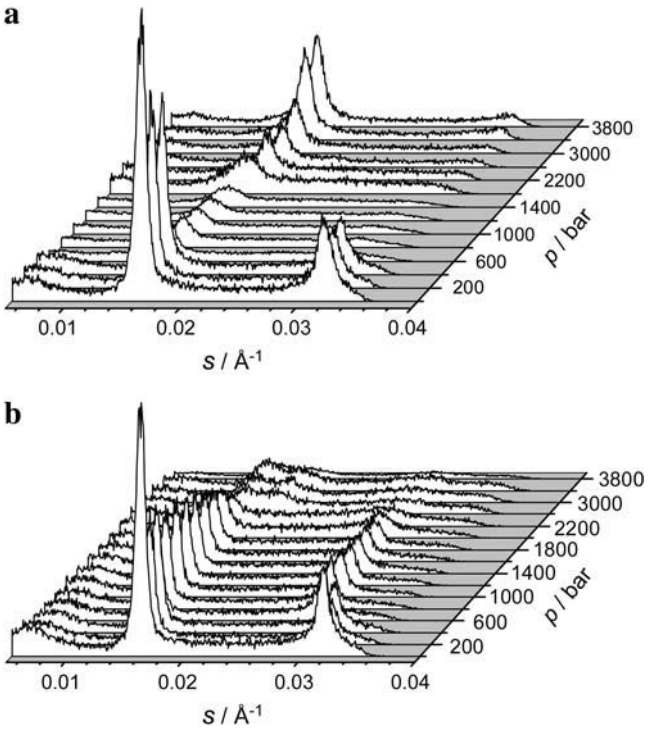

FIGURE 4 SAXS data of (*a*) DMPC (25 wt %) and (*b*) DMPC-2.2 mol % GD in excess water as a function of pressure at $T = 37°C$.

Further SAXS data were taken at 21°C, i.e., starting in the $P_{\beta'}$ gel phase of the lipid bilayer system (data not shown). At ambient pressure, the *d*-spacing is 66 Å at 21°C in pure DMPC, decreases upon pressurization, and at $p \approx 2400$ bar the transition to the $L_{\beta'}$ phase occurs ($d = 59.5$ Å). Up to 3800 bar, the *d*-spacing decreases only slightly (~1 Å) and no indication of a further pressure-induced gel-to-gel phase transition occurs. Addition of, e.g., 2.2 mol GD leads to a drastic swelling of the *d*-spacing up to 70.5 Å at ambient pressure. The *d*-value increases slightly with increasing pressure, and a two-phase region is detected at ~800 bar, which extends up to the full pressure-range covered. The corresponding *d*-spacings of the two gel phases differ by ~13 Å. The smaller one with $d = 60$ Å is similar to that of pure DMPC, suggesting that the increase in *d*-spacing in the second gel phase domains with $d = 73$ Å is due to the insertion of GD. This increase in *d*-spacing is largely due to the increase of the interlamellar water layer (vide infra), which is probably caused by an increase of undulations of the opposing lipid bilayers induced by the GD insertion, leading to a softening of the membrane. Addition of 4.4 mol GD at 21°C leads to a similar scenario (data not shown).

^{2}H-NMR spectroscopy

^{2}H-NMR spectroscopy data were carried out on d_{54}-DMPC and d_{54}-DMPC-GD mixtures in the temperature range from −10°C to 60°C at ambient pressure. We first present the data on pure deuterated 1,2-myristoyl-*sn*-phosphatidylcholine (d_{54}-DMPC) bilayers (Fig. 5). At low temperature, the ^{2}H-NMR spectra of the $L_{\beta'}$ gel phase are visible, as indicated by their strong methylene splittings $\Delta\nu$ of $\sim\pm60$ kHz. An L_c phase is formed only after prolonged cooling at low temperature and is formed from the metastable $L_{\beta'}$ gel phase. Characteristic changes of the spectral shape below ~2°C, in particular the changes in methyl quadrupolar splitting (data not shown, see also below), indicate that partial transformation to the L_c phase has occurred at these low temperatures only, the transformation is still not completed as can be deduced from the still larger splittings of a pure L_c phase (17). At ~13°C, the transformation to the $P_{\beta'}$ ripple gel phase occurs, as indicated by the decrease of the intensity at large $\Delta\nu$ values and the concomitant increase of spectral intensity of the inner methyl groups. A rather sharp transition from the $P_{\beta'}$ gel to the fluid phase occurs at 19.5°C ± 0.5°C (~23.5°C for the nondeuterated lipid) and is readily observable by ^{2}H-NMR as a marked decrease in the width of the spectrum. No methylene resonances can be seen in the gel states, only unresolved curved lineshapes, which are uniquely determined by the particular gel phase state, however. In the L_α phase, an averaged axially symmetric powder pattern composed of many overlapping peaks, corresponding to the various C−D bonds, is seen in the spectrum. Although one cannot resolve every deuteron in the spectrum, we can follow several individual peaks and monitor different regions of the phospholipid molecule, and their segmental order parameters S_{CD} can be determined. The spectral width is ±16.7 kHz at 19.5°C and further decreases with increasing temperature, owing to the increasing chain mobility at higher temperatures.

Incorporation of such a small concentration as 1.1 mol GD leads to marked changes in 2H-NMR spectral properties. Around 4°C, the transition to another gel phase occurs, whose spectral intensity at large $\Delta\nu$ values continuously decreases with increasing temperature. The different spectral shape indicates that the phase if different from a gel phase. Incorporation of GD slightly broadens the main phase transition, so that in the fluid-gel coexistence region the NMR lineshapes show characteristics of both motionally averaged and rigid lattice type spectra between 18°C and 20°C. The NMR spectra of DMPC-2.2 mol GD and DMPC-4.4 mol GD exhibits similar temperature-dependent spectral patterns. Also in these mixtures, two gel phases are observed with a transition temperature of ~4°C. As expected, with increasing GD concentration, the gel-fluid two-phase transition region broadens: For the 2.2 mol GD mixture, it extends from ~16°C to 24°C, and for the lipid mixture with 4.4 mol GD from ~14°C to 26°C.

Fig. 6 *a* displays the temperature dependence of the first spectral moment M_1 of the ^{2}H-NMR spectra. The $L_{\beta'}$ gel phase of DMPC exhibits large M_1 values as high as 30–33 MHz, which is due to the large conformational order of the acyl chains. The splitting of the methyl groups increases

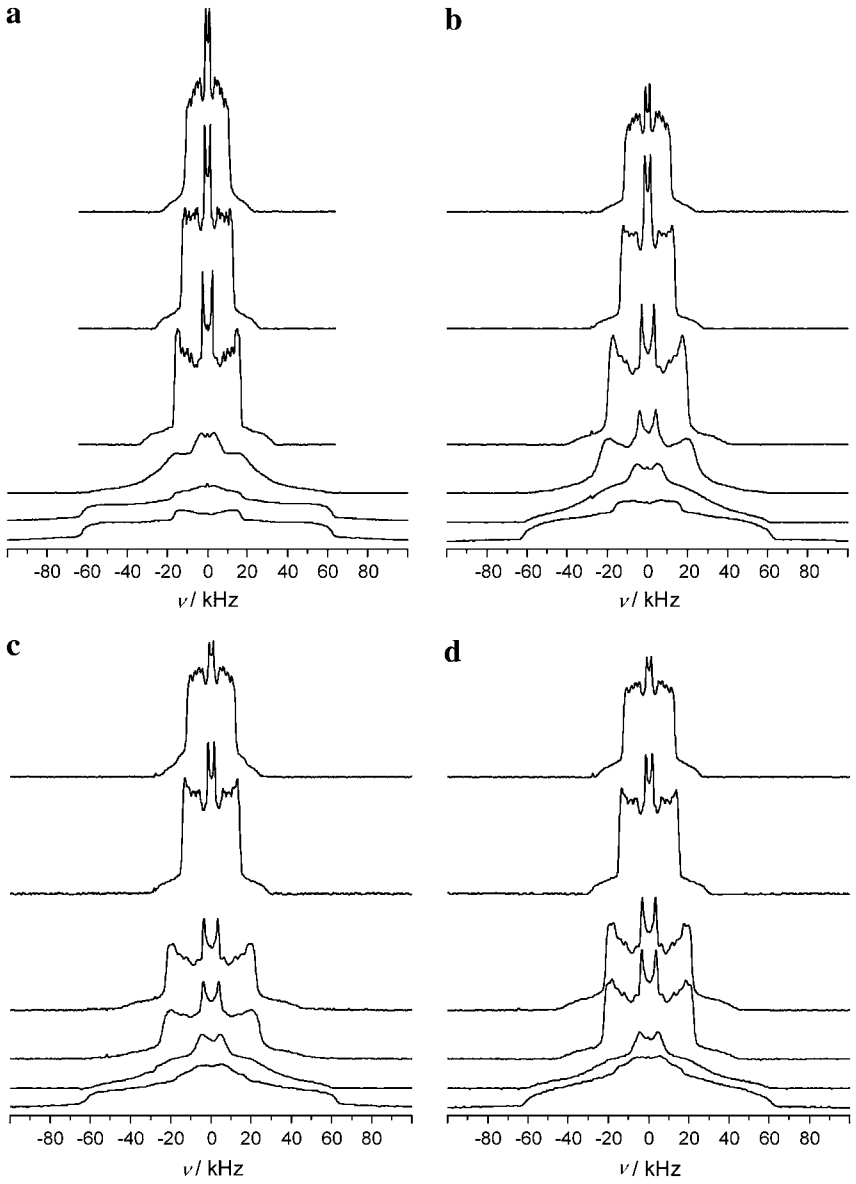

FIGURE 5 ^{2}H-NMR spectra of (*a*) d_{54}-DMPC and (*b*) d_{54}-DMPC-1.1 mol % GD at selected temperatures (from *bottom* to *top*: −7°C, 6.7°C, 18.5°C, 19.4°C, 38.5°C, and 60.6°C); (*c*) d_{54}-DMPC-2.2 mol % GD; and (*d*) d_{54}-DMPC-4.4 mol % GD at selected temperatures (from *bottom* to *top*: −7.5°C, 7.4°C, 18.7°C, 19.7°C, 38.5°C, and 59.7°C).

drastically below ~2°C (27 kHz, data not shown), indicating partial transformation to the L_c phase at these low temperatures. M_1 decreases at the $L_{\beta'}$-to-$P_{\beta'}$ transition at 13°C, and more drastically at the melting temperature of $T_m = 19.5$°C, where values of ~10 kHz are reached in pure d_{54}-DMPC bilayers. Due to further temperature-induced *gauche* conformers and kinks, M_1 decreases further in the fluid phase until $\Delta\nu$ values of 6 kHz are reached at 60°C.

The M_1-data show that incorporation of GD leads to a drastic decrease of the molecular order of the acyl chains in the gel phases, whereas in the fluid phase the mean quadrupolar splitting, and hence the mean order parameter, increases slightly. Above ~4°C, a decrease of M_1 occurs, indicating a marked increase in chain disorder by the insertion of the peptide in this gel phase region. The small and peptide concentration-dependent increase of the M_1 values in the all-fluid phase of the DMPC-GD mixtures point to an increase of conformational order due to the GD partitioning into the fluid lipid bilayer.

To study this effect in greater detail, the segmental order parameters in the liquid-crystalline phase were determined from the quadrupolar splittings (Fig. 7). For some of the methylene groups, the quadrupolar splittings of the *sn*-1 and *sn*-2 chains are slightly different and denoted by index 1 and 2, respectively. As can be clearly seen, the methylene bond order parameters $S_{CD}^{(n)}$ increase markedly in the d_{54}-DMPC-GD mixtures compared to pure d_{54}-DMPC, largely independent of the position in the acyl chain. For example, at 25°C, the mean chain order parameter increases by ~10% and ~30% for the 1.1 and 4.4 mol GD containing lipid mixtures, respectively. The data thus clearly show that GD incorporation into fluid-like DMPC has a significant rigidifying

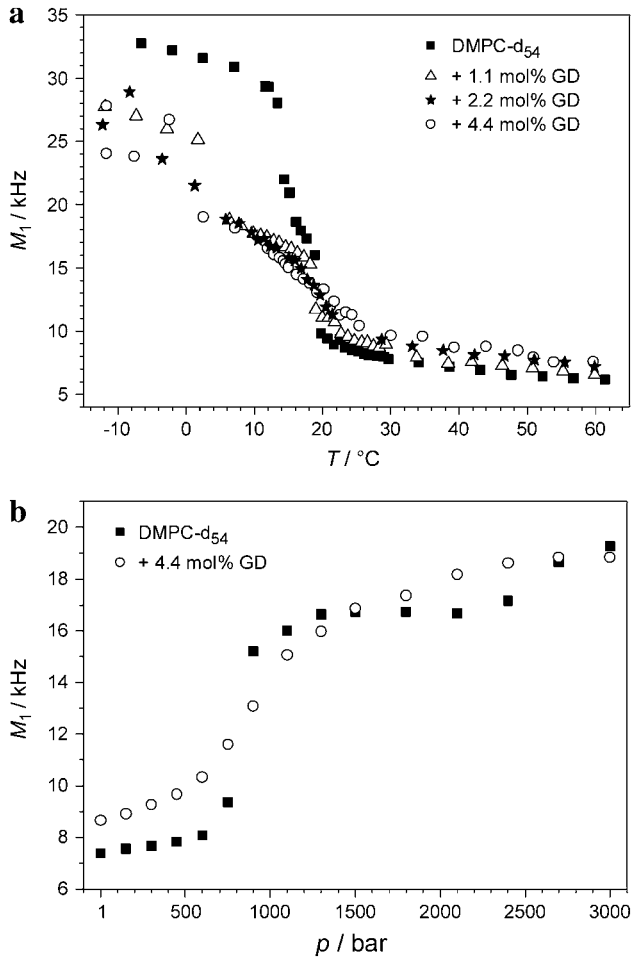

FIGURE 6 (*a*) Temperature dependence of first spectral moment M_1 of the ^{2}H-NMR spectra of d_{54}-DMPC and the d_{54}-DMPC-GD mixtures at ambient pressure. (*b*) Pressure dependence of first spectral moment M_1 of the ^{2}H-NMR spectra of d_{54}-DMPC (*solid symbols*) and the d_{54}-DMPC-4.4 mol % GD mixture at $T = 37$°C.

effect on the chain conformational order in a rather cooperative manner along the whole acyl chain. As expected, the peptide influence on the conformational order decreases with increasing temperature, the effect being more pronounced in the inner part of the lipid bilayer that generally exhibits less conformational order. This effect is particularly pronounced at low temperatures. For example, at $T = 30$°C, we determine an increase of S_{CD} of ~18% in the upper chain region of ~21–27% in the inner chain region and of ~20% for the methyl group in the d_{54}-DMPC-4.4 mol GD mixture with respect to the pure d_{54}-DMPC bilayer. We note that the effects GD incorporation is inducing on the conformational order of the lipid membrane is qualitatively similar to that of the effect of cholesterol incorporation into lipid bilayer systems. In the latter case, the perturbation of the gel phase structure and conformational order is much less pronounced compared to that of GD on a similar molar concentration scale, however (41,42).

From these ^{2}H-NMR spectroscopic data, the mean hydrocarbon chain length D_C and the average chain cross sectional area $\langle A \rangle$ of the lipid molecule can be calculated using the mean-torque model (38) (data not shown). D_C is ~15.7 Å at 20°C in pure fluid DMPC and increases by 1.5 Å by adding 4.4 mol GD, indicating that the hydrophobic mismatch between the fluid lipid and polypeptide length is rather small, and also reflects the rigidifying effect of GD insertion on fluid bilayers. D_c decreases for d_{54}-DMPC as well as for the GD mixtures with increasing temperature between 30°C and 60°C at a rate of $dD_c/dT \approx -0.05$ Å/°C. The average chain cross sectional area $\langle A \rangle$ of d_{54}-DMPC is ~55 ± 1 Å^2 at 20°C, which agrees well with literature data (28,38,43), and decreases to 50 Å^2 in the DMPC-4.4 mol GD mixture at that temperature. The temperature dependence of the mean chain cross sectional area in the fluid phase above ~30°C increases linearly up to ~60°C and, within the accuracy of the experiment, is independent of the GD concentration ($d\langle A \rangle/dT \approx 0.32$ Å^2/°C).

The characteristic changes of D_C and $\langle A \rangle$ approaching the fluid-to-gel transition are characteristic of the pseudocritical character of the transition, which has been extensively discussed in the literature (43–45). A nonlinear increase (swelling) of the lamellar lattice constant has been attributed to a drop of the bilayer bending rigidity in the vicinity of the main transition temperature, which, owing to bilayer undulations, enhances the steric repulsion of opposing bilayers, thus increasing the interbilayer spacing. Our SAXS and ^{2}H-NMR data indicate that the critical swelling (~4 Å) is only partially (~30%) due to an increase in lipid length. Remarkably, this behavior seems to be slightly more pronounced for the DMPC-GD mixtures.

Pressure-dependent ^{2}H-NMR measurements on d_{54}-DMPC and the d_{54}-DMPC-GD mixtures were carried out at 20°C and 37°C up to pressures of ~3 kbar. We will mainly focus on the 37°C data here (Fig. 8). The pressure-induced fluid-gel main phase transition of pure d_{54}-DMPC at 37°C is identified at a pressure of ~800 bar as an increase of the first spectral moment M_1, which is shown in Fig. 7 *b*. Also observed at this pressure is a drastic change in the lineshape from a motionally averaged spectrum in the liquid-crystalline phase to a gel phase type ^{2}H-NMR spectrum (Fig. 8). Further increase of pressure leads to a significant change in the lineshape above ~1800 bar, whereas the first moment shows no marked change in that pressure range. At these pressures, the $P_{\beta'}$ gel phase transforms to the $L_{\beta'}$ gel phase. Above 2600 bar, a further gel-to-gel transition is detected.

Incorporation of GD into the lipid bilayer drastically broadens the main phase transition, as can be clearly seen in the change of the first spectral moment with pressure (Fig. 7 *b*). The ^{2}H-NMR lineshapes of the d_{54}-DMPC-4.4 mol GD mixture are markedly different. Above 1100 bar, the ^{2}H-NMR spectra are indicative of formation of a pressure-induced gel phase. At ~2200 bar, a further gel-to-gel transition is indicated in the ^{2}H-NMR spectra. The spectra can

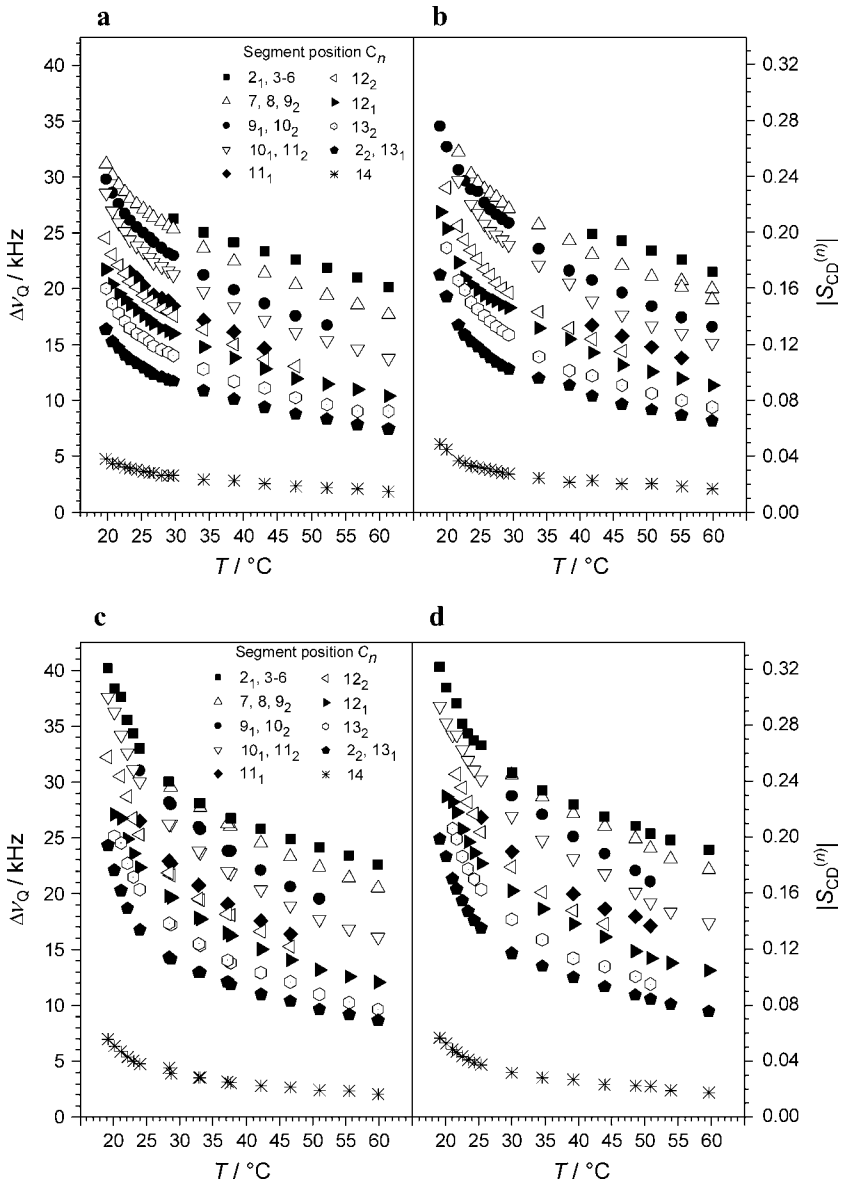

FIGURE 7 Temperature dependence of the measured quadrupolar splittings and the segmental order parameter profiles of (*a*) pure d_{54}-DMPC (25 wt %) dispersions and of the d_{54}-DMPC-GD mixtures: (*b*) 1.1 mol % GD, (*c*) 2.2 mol % GD, and (*d*) 4.4 mol % GD.

be viewed as a superposition of two gel-type spectra with different degrees of order. This is in agreement with the M_1 data, which reach a plateau value above ~2.2 kbar. In particular from the concomitant SAXS data we may conclude that a gel-gel two-phase region is formed at these high pressures.

The pressure dependence of the segmental C-D order parameters in the fluid phase at 37°C is depicted in Fig. 9. As expected, the chain order parameter values increase with increasing pressure, in particular at the inner methylene segments and, interestingly, more rapidly approaching the pressure-induced fluid-to-gel phase transition region. For example, the order parameter of the chains increases by ~10% at ambient pressure and by ~30% for d_{54}-DMPC-4.4 mol GD at $p = 600$ bar. As expected, the order parameter increases less in the plateau region (in the upper part of the acyl chains) than in the inner part of the lipid bilayer.

The hydrocarbon chain length D_C of the pure d_{54}-DMPC monolayer at 37°C increases from 14.1 Å at 1 bar to 15.0 Å at 750 bar (data not shown). For the mixture with 4.4 mol GD, D_C increases from 14.8 Å at 1 bar to a significantly higher value of 16.8 Å at 750 bar. These data verify that the observed small increase of the *d*-spacings upon incorporating of GD into the fluid DMPC bilayer is essentially due to a stretching of the lipid's acyl chains. The average chain cross sectional area $\langle A \rangle$ at 37°C decreases concomitantly from ~63 $Å^2$ in pure DMPC at 1 bar to ~56 $Å^2$ at 750 bar. Adding 4.4 mol GD to the DMPC bilayer yields corresponding values of 60 $Å^2$ at ambient pressure (decrease of 5%) and 50 $Å^2$ at 750 bar (decrease of 12%), respectively.

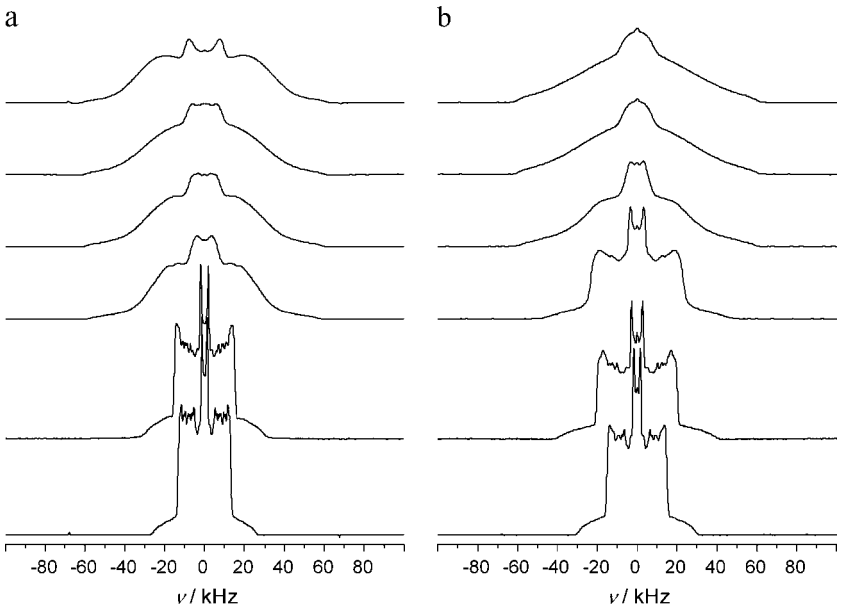

FIGURE 8 ^{2}H-NMR spectra of (*a*) d_{54}-DMPC and (*b*) d_{54}-DMPC-4.4 mol % GD at selected pressures (from *bottom* to *top*: 1, 750, 900, 1500, 2400, and 3000 bar) for $T = 37°C$.

The nonlinear increase of the *d*-spacings in the fluid phase when approaching the fluid-gel transition boundary, which starts ~300 bar before the phase boundary is reached (Fig. 5), is partially mirrored in the corresponding behavior of the segmental order parameter values and the mean lipid chain length (Fig. 9). A significant ''anomalous'' swelling of the interlamellar *d*-spacing due to a solely increasing swelling of the interlamellar water layer is therefore not the case in this pressure-induced fluid-to-gel transition of DMPC. As revealed from the pressure-dependent lattice spacings and D_c data, this is partially (30%) due to a lengthening of the lipid chains. As mentioned before, such anomalous swelling, i.e., nonlinear increase in *d*-spacing when approaching the main liquid-crystalline-to-gel transition, has been observed in ambient pressure experiments in a series of phospholipid systems ((43–45) and references therein) and is generally attributed to a pretransitional behavior typical for weak first-order phase transitions. Hence, for both the temperature- and pressure-induced fluid-to-gel transition, a similar pseudocritical transitional behavior is observed (though it seems to be slightly damped upon pressurization), which, interestingly, is even more pronounced upon incorporation of the peptide.

Measurements have also been carried out at 20°C (data not shown). For the pure lipid system, the fluid-to-$P_{\beta'}$ transition occurs at ~100 bar, and a further transition is detected at 900 bar where the $L_{\beta'}$ gel phase appears, as indicated by its characteristic spectral lineshape. For the d_{54}-DMPC-4.4 mol GD mixture, the transition from a fluid-gel coexistence region to a pressure-induced all-gel state is much broader. The latter is stable up to ~900 bar. At 1200 bar, a further spectral change indicates the transition to a gel-gel coexistence region.

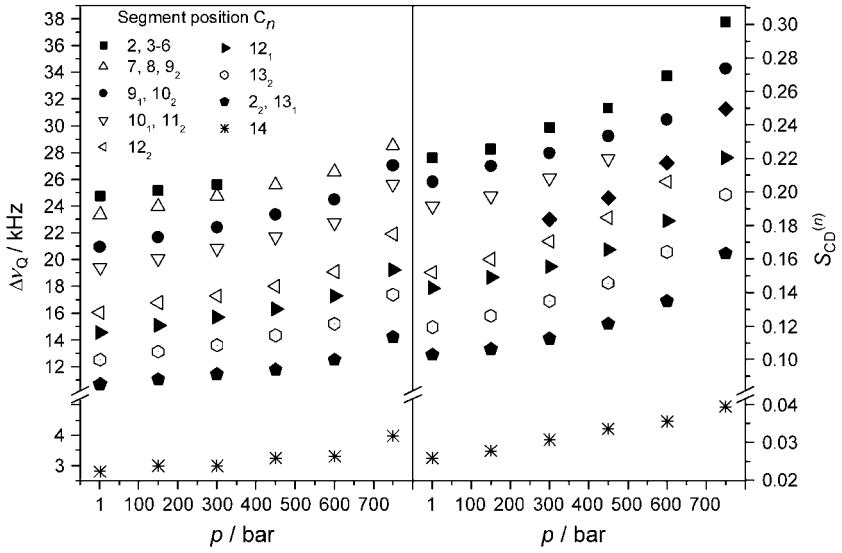

FIGURE 9 Temperature dependence of the measured quadrupolar splittings and the segmental order parameter profiles of pure d_{54}-DMPC (25 wt %) dispersions (*left*) and the d_{54}-DMPC-4.4 mol % GD mixture (*right*) at $T = 37°C$.

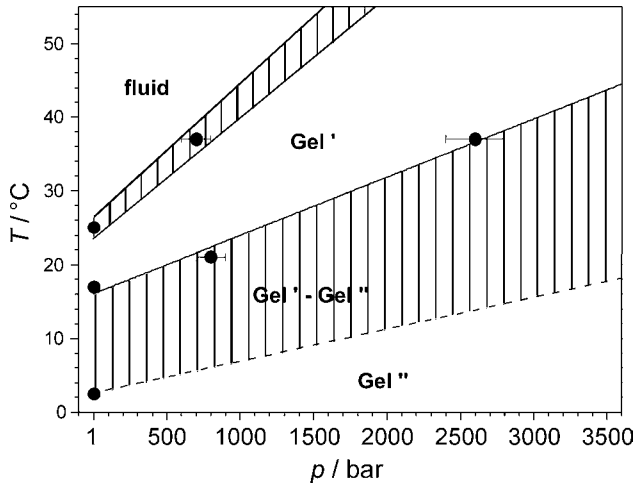

FIGURE 10 Tentative T,p-phase diagram of DMPC-2.2 mol % GD in excess water as obtained from the SAXS (·) and FTIR spectroscopy studies. The slope of the lower gel phase boundary is tentative only (*dashed line*).

We conclude that gramicidin insertion clearly has a significant influence on the lipid bilayer structure and temperature, pressure-phase behavior of DMPC bilayers. Together with recently published results from FTIR spectroscopic studies (18), we are able to construct a tentative p,T-phase diagram for the DMPC-2.2 mol GD mixture from the SAXS data up to pressures of 3500 bar, which is shown in Fig. 10. Upon gramicidin insertion, a rather small fluid-gel coexistence region is formed and two pressure-induced gel phases (Gel′, Gel″) are induced, which are different from those of the pure lipid bilayer system and which separate at low temperatures/high pressures. Only the fluid-/fluid-gel phase boundary occurs at a similar place and has a similar dT/dp slope as the fluid/gel ($P_{\beta'}$) transition of pure DMPC bilayers. The ^{2}H-NMR spectroscopy data on the deuterated DMPC-GD bilayer system are, taking the isotope effect on the transition temperatures into account, in good agreement with these data.

Financial support from the Deutsche Forschungsgemeinschaft and the Fonds der Chemischen Industrie is gratefully acknowledged.

REFERENCES

1. Yeagle, P. L., editor. 2005. The Structure of Biological Membranes. CRC Press, Boca Raton, FL.
2. Jensen, M. Ø., and O. G. Mouritsen. 2004. Lipids do influence protein function—the hydrophobic matching hypothesis revisited. *Biochim. Biophys. Acta.* 1666:205–226.
3. Lipowski, R., and E. Sackmann, editors. 1995. Structure and Dynamics of Membranes, Vols. 1A and 1B. Elsevier, Amsterdam, The Netherlands.
4. Mouritsen, O. G. 2005. Life as a Matter of Fat. The Emerging Science of Lipidomics. Springer, Heidelberg, Germany.
5. Balny, C., P. Masson, and K. Heremans. 2002. High pressure effects on biological macromolecules: from structural changes to alteration of cellular processes. *Biochim. Biophys. Acta.* 1595:3–10.
6. Ludwig, H., editor. 1998 Advances in High Pressure Bioscience and Biotechnology. Springer-Verlag, Heidelberg, Germany.
7. Winter, R., editor. 2003. Advances in High Pressure Bioscience and Biotechnology II. Springer-Verlag, Heidelberg, Germany.
8. Winter, R., and W. Dzwolak. 2004. Temperature-pressure configurational landscape of lipid bilayers and proteins. *Cell. Mol. Biol.* 50:397–417.
9. Winter, R., and W. C. Pilgrim. 1989. A SANS study of high pressure phase transitions in model biomembranes. *Ber. Bunsenges. Phys. Chem.* 93:708–717.
10. Czeslik, C., O. Reis, R. Winter, and G. Rapp. 1998. Effect of high pressure on the structure of dipalmitoylphosphatidylcholine bilayer membranes: a synchrotron-x-ray diffraction and FTIR spectroscopy study using the diamond anvil technique. *Chem. Phys. Lipids.* 91: 135–144.
11. Winter, R., and C. Czeslik. 2000. Pressure effects on the structure of lyotropic lipid mesophases and model biomembrane systems. *Z. Kristallogr.* 215:454–474.
12. Jonas, J., editor. 1991, High Pressure NMR. Springer-Verlag, Berlin.
13. Peng, X., A. Jonas, and J. Jonas. 1995. One and two dimensional ^{1}H-NMR studies of pressure and tetracaine effects on sonicated phospholipid vesicles. *Chem. Phys. Lipids.* 75:59–69.
14. Braganza, L. F., and D. L. Worcester. 1986. Hydrostatic pressure induces hydrocarbon chain interdigitation in single-component phospholipid bilayers. *Biochemistry.* 25:2591–2596.
15. Fiech, D. C., B. B. Bonev, and M. R. Morrow. 1998. Effect of pressure on dimyristoylphosphatidylcholine headgroup dynamics. *Phy. Rev. E.* 57:3334–3343.
16. Bonev, B. B., and M. R. Morrow. 1998. ^{2}H NMR studies of dipalmitoylphosphatidylcholine and dipalmitoylphosphatidylcholine-cholesterol bilayers at high pressure. *Can. J. Chem.* 76:1512–1515.
17. Bonev, B. B., and M. R. Morrow. 1997. Effect of pressure on the dimyristoylphosphatidylcholine bilayer main transition. *Phys. Rev. E.* 55:5825–5833.
18. Zein, M., and R. Winter. 2000. Effect of temperature, pressure and lipid acyl-chain length on the structure and phase behaviour of phospholipid-gramicidin bilayers. *Phys. Chem. Chem. Phys.* 2:4545–4551.
19. Chong, P. L., P. A. Fortes, and D. M. Jameson. 1985. Mechanisms of inhibition of (Na,K)-ATPase by hydrostatic pressure studied with fluorescent probes. *J. Biol. Chem.* 260:14484–14490.
20. Janosch, S., E. Kinne-Saffran, R. K. H. Kinne, and R. Winter. 2003. Inhibition of Na^+, K^+-ATPase by hydrostatic pressure. *In* Advances in High Pressure Bioscience and Biotechnology II. R. Winter, editor. Springer-Verlag, Heidelberg, Germany. 215–219.
21. Scarlata, S. 2005. Determination of the activation volume of PLCβ by G$\beta\gamma$-subunits through the use of high hydrostatic pressure. *Biophys. J.* 88:2867–2874.
22. Wallace, B. A. 1990. Gramicidin channels and pores. *Annu. Rev. Biophys. Biomol. Struct.* 19:127–157.
23. Koeppe II, R. E., and O. S. Andersen. 1996. Engineering the gramicidin channel. *Annu. Rev. Biophys. Biomol. Struct.* 25:231–258.
24. Chadwick, D. J., and G. Cardew, editors. 1999. Gramicidin and Related Ion Channel-Forming Peptides. Novartis Foundation Symposium 225. John Wiley & Sons, New York.
25. Koert, U. 2005. Synthetic ion channels: functional analysis and structural studies. *Phys. Chem. Chem. Phys.* 7:1501–1506.
26. Townsley, L. E., W. A. Tucker, S. Sham, and J. F. Hinton. 2001. Structures of gramicidins A, B, and C incorporated into sodium dodecyl sulfate micelles. *Biochemistry.* 40:11676–11686.
27. Cevc, G., editor. 1993. Phospholipids Handbook. Marcel Dekker, New York.
28. Nagle, J. F. 1993. Area/lipid of bilayers from NMR. *Biophys. J.* 64: 1476–1481.
29. Katsaras, J., and V. A. Raghunathan. 1995. Molecular chirality and the ''ripple'' phase of phosphatidylcholine multilayers. *Phys. Rev. Lett.* 74: 2022–2025.
30. Katsaras, J., S. Tristram-Nagle, Y. Liu, R. L. Headrick, E. Fontes, P. C. Mason, and J. F. Nagle. 2000. Clarification of the ripple phase of

lecithin bilayers using fully hydrated, aligned samples. *Phys. Rev. E.* 61:5668–5677.

31. Eisenblätter, J., A. Zenerino, and R. Winter. 2000. High pressure ^{1}H-NMR on model biomembranes: a study of the local anaesthetic tetracaine incorporated into POPC lipid bilayers. *Magn. Reson. Chem.* 38:662–667.
32. Winter, R. 2003. High pressure NMR studies on lyotropic lipid mesophases and model biomembranes. *Ann. Rep. NMR Spectr.* 50:163–200.
33. Seelig, J. 1977. Deuterium magnetic resonance: theory and application to lipid membranes. *Q. Rev. Biophys.* 10:353–418.
34. Seelig, J., and P. M. MacDonald. 1987. Phospholipids and proteins in biological membranes. Deuterium NMR as a method to study structure, dynamics, and interactions. *Acc. Chem. Res.* 20:221–228.
35. Davis, J. H. 1983. The description of membrane lipid conformation, order and dynamics by ^{2}H-NMR. *Biochim. Biophys. Acta.* 737:117–171.
36. Davis, J. H. 1989. Deuterium nuclear magnetic resonance and relaxation in partially ordered systems. *Adv. Magn. Reson.* 13:195–223.
37. Petrache, H. I., K. Tu, and J. F. Nagle. 1999. Analysis of simulated NMR order parameters for lipid bilayer structure determination. *Biophys. J.* 76:2479–2487.
38. Petrache, H. I., S. W. Dodd, and M. F. Brown. 2000. Area per lipid and acyl length distributions in fluid phosphatidylcholines determined by ^{2}H NMR spectroscopy. *Biophys. J.* 79:3172–3192.
39. Böttner, M., D. Ceh, U. Jacobs, and R. Winter. 1994. High pressure volumetric measurements on phospholipid bilayers. *Z. Phys. Chem.* 184:205–218.
40. Seemann, H., and R. Winter. 2003. Volumetric properties, compressibilities and volume fluctuations in phospholipid-cholesterol bilayers. *Z. Phys. Chem.* 217:831–864.
41. Miao, L., M. Nielsen, J. Thewalt, J. H. Ipsen, M. Bloom, M. J. Zuckermann, and O. G. Mouritsen. 2002. From lanosterol to cholesterol: structural evolution and differential effects on lipid bilayers. *Biophys. J.* 82:1429–1444.
42. Vist, M. R., and J. H. Davis. 1990. Phase equilibria of cholesterol/dipalmitoylphosphatidylcholine mixtures: ^{2}H nuclear magnetic resonance and differential scanning calorimetry. *Biochemistry.* 29: 451–464.
43. Lemmich, J., K. Mortensen, J. H. Ipsen, T. Honger, R. Bauer, and O. G. Mouritsen. 1995. Pseudocritical behavior and unbinding of phospholipid bilayers. *Phys. Rev. Lett.* 75:3958–3961.
44. Mason, P. C., J. F. Nagle, R. M. Epand, and J. Katsaras. 2001. Anomalous swelling in phospholipid bilayers is not coupled to the formation of a ripple phase. *Phys Rev. E.* 63:030902.
45. Harroun, T. A., M. P. Nieh, M. J. Watson, V. A. Raghunathan, G. Pabst, M. R. Morrow, and J. Katsaras. 2004. Relationship between the unbinding and main transition temperatures of phospholipid bilayers under pressure. *Phys. Rev. E.* 69:031906.